

SHEAR DEFORMATION AND MATERIAL PROPERTIES OF POLYMER-MODIFIED ASPHALT

*Zora Vlachovicova, Jiri Stastna, Daryl MacLeod and Ludo Zanzotto
corresponding author*

2500 University Drive, Calgary, AB, Canada, T2N 1N4, zvlachov@ucalgary.ca

Received July 27, 2005; accepted December 15, 2005

Abstract

The aim of this article is the comparison of flow properties of base and polymer-modified asphalts in different experimental modes. Various concentrations of polymers were added to base asphalt. Effect of the modification was observed and peculiar behaviour (noticed especially in steady state measurements) was modeled.

When polymer-modified asphalts are studied in small amplitude oscillations, the obtained dynamic material functions are not very different qualitatively from those of conventional asphalts. The situation is changed when the same materials are studied in the strong steady shear regime (with a broad range of shear rates). In the blends of soft (conventional) asphalt with styrene-butadiene-styrene (SBS) and ethylene-vinyl-acetate (EVA) copolymers, the shear viscosity function exhibits a typical non-Newtonian behaviour at some temperatures. Then, at other temperatures (depending on the polymer and its concentration), the viscosity function has a double-step shear-thinning behaviour and, in some cases, even a small shear-thickening region can be observed. This unusual behaviour is caused by rearrangement of a polydomain structure and detachment of flexible chains in polymer-modified asphalt. The resulting network is responsible for the nonlinear behaviour of polymer-modified asphalts. It is shown that the generalized rubber-like liquid model can describe this nonlinear behaviour of polymer-modified asphalts well.

Key words: Asphalt; polymer modification; liquid crystals; nonlinear models

1. Introduction

It is generally agreed that asphalt has a colloidal nature. It can be fractionated by solvent fraction methods or by thin layer chromatography into: saturates, aromatics, resins and asphaltenes (SARA). The polarity and molecular weight of these fractions increases in the respective order of SARA^[1]. It is difficult to define the asphalt molecule: the working model of such a molecule is "a system of repeating units of similar composition"^[2]. X-ray diffractograms of asphaltenes showed a characteristic pattern of aromatic sheets (width, 9-15 Å) stacked in layers (thickness, 16-24 Å)^[3]. Dickie et al.^[2] found evidence for large associations of asphaltene particles to gather into clusters. According to Lian et al.^[1], an aggregate of asphaltene particles with adsorbed resins can form a supermicelle (10-20 nm). These can coalesce into giant supermicelles (200-2000nm), and eventually grow into a liquid crystal (~100 000nm). The colloidal structure of asphalt and its time evolution are controlled by the chemistry of its compounds, especially by the asphaltenes/resin ratio. The majority of asphalt colloidal particles have a characteristic dimension of 10-15nm, and they are usually classified as multipolymers (i.e. polycondensates of random polymers with a variety of building blocks).

Yen^[4] used infrared spectra for the study of the charge-transfer characteristics of polyaromatic molecules and associations in asphalt. Four bands located approximately at 865, 815, 760 and 730 cm⁻¹ were observed in asphalt. The first three bands correspond to aromatic C-H out of plane bending vibrations. The fourth band, occurring as a shoulder at 731-720 cm⁻¹, was assigned to in-plane methylene rocking vibrations of paraffinic nature^[5]. By studying the frequency shifts of infrared spectra of asphalt in various solvents and complexing reagents, Yen concluded that colloidal characteristics of asphalt might be explained through the charge-transfer nature of aromatic systems of asphaltic macrostructure.

The study of the internal structure of asphalt is made extremely difficult by the very high viscosity of asphalt and the complexity of its components. The studies have to be performed in a diluted solvent, which inadvertently changes the structure of the part of asphalt with either the largest molecular weight or the greatest polarity. Thus, the decisive evidence of the internal structure of asphalt is still lacking.

When used for paving applications, asphalt from crude oil distillation sometimes does not provide efficient resistance towards factors influencing the quality of the pavement (temperature extremes, imposed stress, accumulated strain, etc.). In order to enhance asphalt binder properties and widen the service temperature^[6], asphalt is often modified by various additives (different fillers, fibers, polymers, etc.). Polymer modification improves mechanical properties, decreases thermal susceptibility and permanent deformation (rutting), and increases resistance to low-temperature cracking. The most commonly used additives are copolymers, such as SBS, EVA, etc. The wide use of this type of polymer for modification is due to their thermoplastic nature at higher temperatures and their ability to form networks upon cooling. It has been shown^[7,8] that rheological properties may change dramatically by modification of the base asphalt by these types of polymers.

2. Materials and Methods

Materials

In this study, a soft base asphalt (200/300 Pen grade) was modified with styrene-butadiene-styrene (SBS) and ethylene-vinyl-acetate (EVA) polymers. Their concentration in the resulting polymer-modified asphalts (PMA) varied from 1 to 8%, by weight. The SBS was radial with star architecture and had an average of 3.5 arms. Its molecular weight was 150000 and the B/S ratio was 70/30.

SBS polymers consist of styrene-butadiene-styrene tri-block chains and have a two-phase morphology, where the spherical domains are formed by the polystyrene blocks within a matrix of polybutadiene. Polystyrene has a glass transition temperature of about 95°C, and the elastomeric blocks of rubber have a glass transition temperature of about -80°C. The extreme difference in glass transition temperatures and the fact that SBS exhibits physical crosslinking make this polymer very interesting for asphalt modification.

The EVA copolymer used for asphalt modification in this study contained 25% of vinyl acetate. EVA copolymer is created by the insertion of vinyl acetate units into the polyethylene chain, introducing structural irregularities and causing a decrease in its crystallization ability. As a result, as the level of vinyl acetate in copolymer increases, the level of crystallinity reduces from about 60% to 10%. As the degree of crystallinity decreases, the number of defects in the crystals increases; therefore, the melting temperature can change from about 100°C, for very low acetate content, to about 60°C corresponding to an acetate content around 30% by weight. If the operating conditions are properly chosen, the EVA-modified asphalt contains a physical network where the crosslinking units are the crystallites rich in ethylene units^[9].

Instruments

The studies discussed in this article included FTIR spectrometry, viscosity and frequency sweep measurements. These were performed on two types of instruments. The FTIR spectra were captured by a Nexus 670 FT-IR spectrometer from Thermo Nicolet. The other two types of measurements were accomplished with the help of an ARES 33-A rheometer (manufactured by TA Instruments), which is a controlled strain rheometer. In this type of instrument, the desired strain is set and the stress as an output is measured.

Methods

The samples for FTIR spectrometry were prepared by dissolution of a small amount of asphalt in tetrahydrofuran (THF). This solution was then applied to NaCl plate to form a film thick enough so that the absorbance at 1376 cm⁻¹ (symmetrical deformation vibration of the CH₃ group) would fall between 0.4 and 0.6.

The samples for rheological measurements were prepared by the melting of the asphalt in a small container. The melted asphalt was then poured into rubberized moulds to form asphalt discs in the final

form. After reaching the ambient temperature, the samples were moved into the freezer and then used for measurement.

The viscosity of the asphalt was tested in a cone and plate geometry setup with the cone/plate (CP) diameters being 25 or 50 mm (cone angle 4°), depending on the temperature used for the measurement. The larger CP diameter was used for measurements at temperatures higher than 60°C.

When working in the dynamic mode of the instrument (frequency sweep measurements), torsional bar geometry was chosen for measurements at subzero temperatures. In this mode, the strain applied to the sample was very small (again, depending on the temperature), and the frequency was changed from 0.01 to 15 Hz. In the steady mode (viscosity measurements), the shear rates applied on the sample ranged from 5×10^{-4} to 100 s^{-1} .

The temperature interval in the dynamic measurements was from -40°C to 90°C; in steady shear measurements, it was 40°C-90°C (in some cases, up to 130°C).

3. Results and Discussion

Fourier Transform Infrared (FTIR) Spectroscopy

Conventional asphalt is a material with a complicated structure, and there are number of theories about the possible composition of such a complex substance. Generally, it has been agreed that asphalt is a colloidal material, where asphaltenes are stabilized by the layer of resins, which are dispersed in the oily phase (saturates, naphthene aromatics). When polymer is added into this structure, the task of a clear explanation of the intermolecular relationships becomes even more challenging. This is the reason why a series of rheological tests, accompanied by methods of physical chemistry, etc., is necessary for finding the best possible modifier in order to create an asphalt binder with improved engineering properties.

One of the methods reported here is FTIR spectroscopy. Figures 1 and 2 portray the infrared spectra of asphalts used in this study. Figure 1 displays spectra that compare the base asphalt with the different concentrations of the SBS PMA. The typical peaks for asphalts, identified by Yen [4], are clearly visible in the region between 900 cm^{-1} and 700 cm^{-1} . The characteristic bands for SBS polymer are situated around 966 cm^{-1} and 698 cm^{-1} [10]. As seen from the spectra, these peaks border four typical asphalt peaks from both sides. The increasing concentration of polymer is clearly seen in these two bands, as well as their absence in the base asphalt.

The characterization of the EVA PMA and its comparison with Elvax© polymer (pure EVA polymer) and with base asphalt are presented in Figure 2, where the FTIR spectra are shown. There are two characteristic bands for the EVA copolymer, and their location is around 1736 and 1242 cm^{-1} . Once again, as in the case of SBS-modified asphalts, the different concentrations of EVA in asphalt can be seen in these peaks. The typical asphalt peaks are again clearly seen.

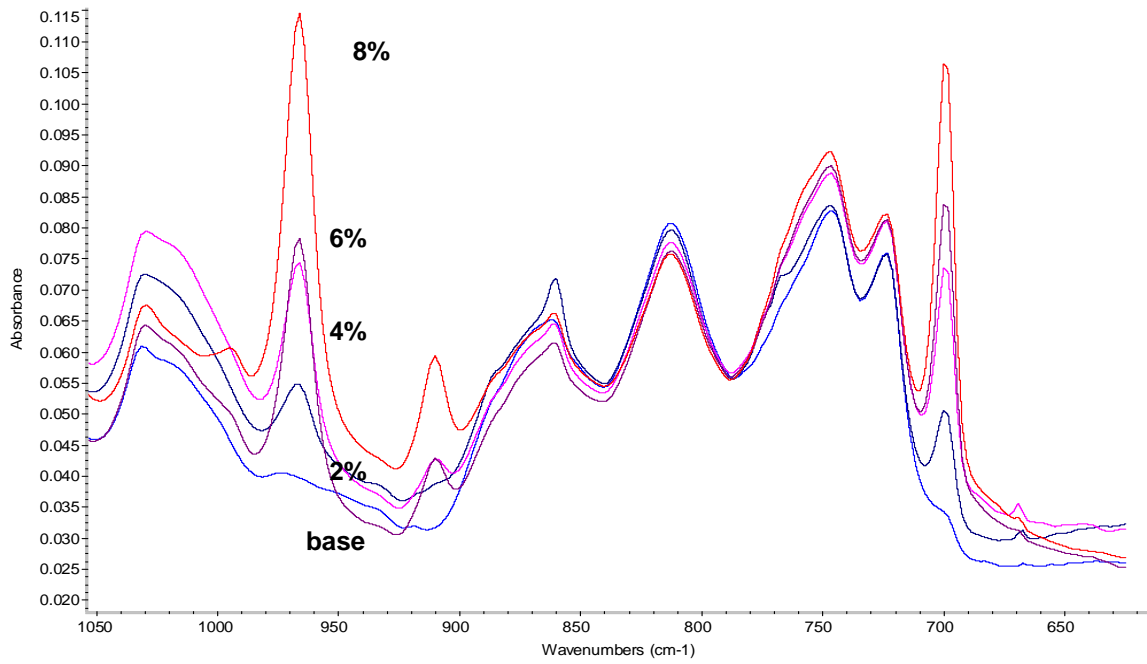


Figure 1: Infrared spectra: base asphalt and different concentrations of SBS in PMA.

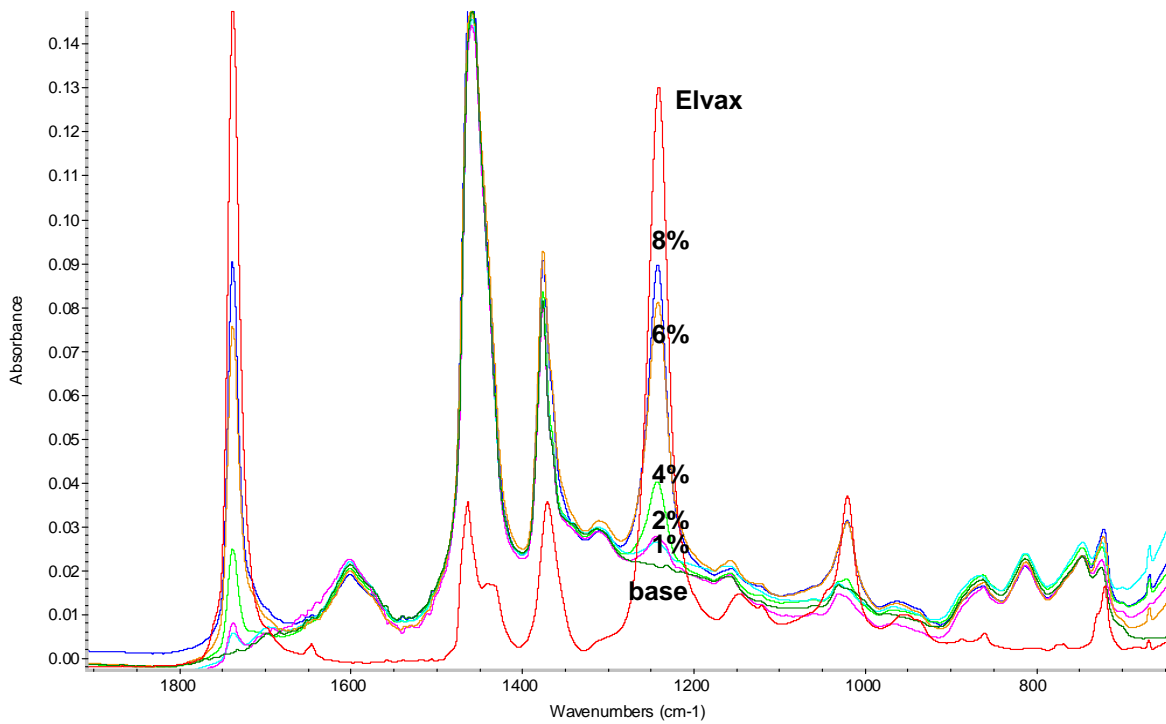


Figure 2: Infrared spectra: base asphalt and different concentrations of EVA in PMA and Elvax polymer.

Dynamic Oscillation Characterization

The linear viscoelastic properties of asphalt are often characterized by performing small amplitude oscillations on the tested asphalt sample [11]. From the components of the complex modulus $G^*(\omega) = G'(\omega) + iG''(\omega)$, the relaxation spectrum of the tested material can be determined. In the case of Maxwell relaxation modes, the storage (elastic) (G') and the loss (viscous) (G'') modulus are directly related to the discrete relaxation spectrum $\{g_i, \lambda_i\}$ [12]:

$$G'(\omega) = \sum_i \frac{g_i (\omega \lambda_i)^2}{1 + (\omega \lambda_i)^2}, G''(\omega) = \sum_i \frac{g_i (\omega \lambda_i)}{1 + (\omega \lambda_i)^2}. \quad (1)$$

Other linear viscoelastic functions can be calculated by knowing the relaxation spectrum^[12].

Figure 3 displays the dynamic master curve (after superposition of dynamic data measured at temperatures from -70°C to 90°C) of the 8% SBS PMA. The bar under the figure shows the temperatures that correspond to the reduced frequencies. The measured data are represented by symbols, and the lines represent the fit to equations in (1). The biggest problem is usually the construction of smooth master curves (especially for asphalt with a high content of polymer). The overall fit to the experimental data is satisfactory, except at 50°C and very low temperatures. It is not yet clear if the latter represents another transition, or if it is an artifact of the testing geometry. The software (IRIS,^[13]) had no problem fitting even complicated data, such as shown in Figure 3.

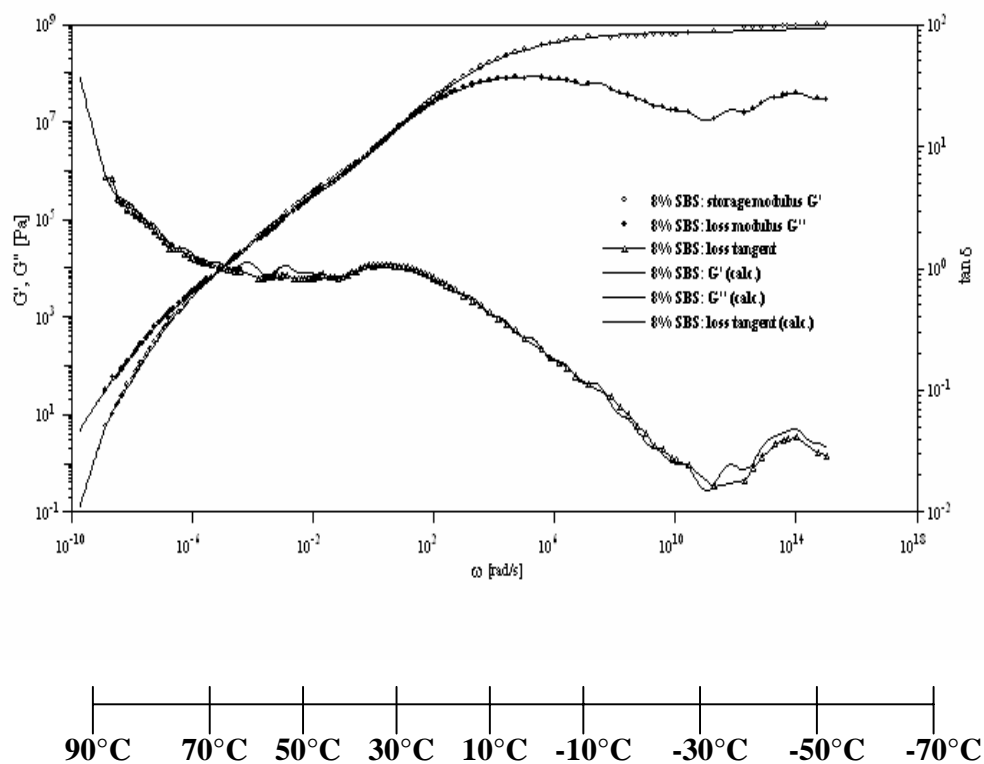


Figure 3: Master curve, 8% SBS PMA; $T_r=0^\circ\text{C}$.

Steady Shear Viscosity

The classic non-Newtonian behaviour of the base asphalt is portrayed in Figure 4 – note the a long zero-shear viscosity plateau. When a certain critical shear rate is reached, sharp shear thinning begins. The higher the temperature is, the higher the critical shear rate. For temperatures up to 60°C, the critical shear rate is captured in Figure 4. In this asphalt, a critical shear rate of more than 100s⁻¹ would be needed to achieve the shear thinning at the highest temperatures.

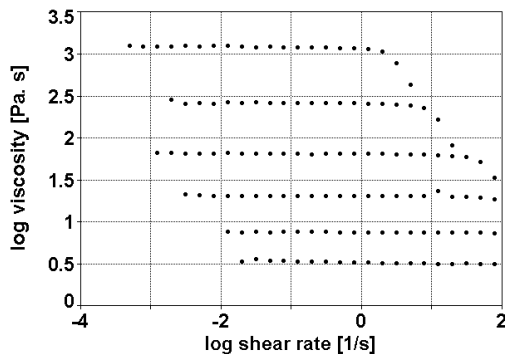


Figure 4: Viscosity function, base asphalt; T= 40°C, 50°C, 60°C, 70°C, 80°C, 90°C.

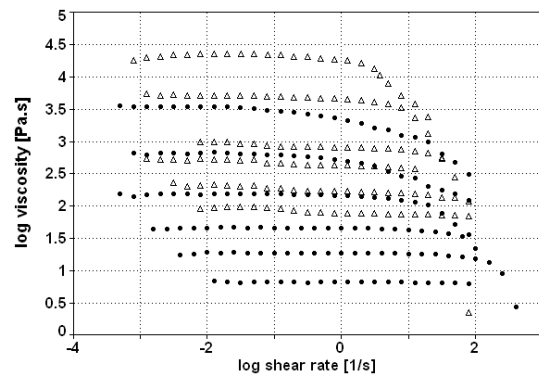


Figure 5: Viscosities comparison, 2% SBS PMA (●), 2% EVA PMA (Δ); T= 40°C, 50°C, 60°C, 70°C, 80°C, 90°C.

The situation is different when asphalts are modified with EVA or SBS copolymers. The viscosity function starts to change gradually with increasing concentrations of the added polymer. Figure 5 represents this scenario, where 2% SBS PMA and 2% EVA PMA are displayed. The transition between Newtonian and non-Newtonian behaviour is not as sharp as in the case of the base asphalt.

The effect of polymer modification starts to be noticeable with the addition of 4% of the polymer. Figure 6 confirms this, as it shows the viscosity function of the 4% SBS PMA at different temperatures. It is obvious that the shape of the viscosity curve is different from previous figures. At 50°C and 60°C, it does not go through only one, but two non-Newtonian shear-thinning regions. Peculiar behaviour is seen in Figure 7, where the 4% SBS PMA and the 4% EVA PMA are compared at 50°C and 60°C. The viscosity of the 4% SBS PMA at 50°C shows a small shear thickening, with its peak at around 0.05 s⁻¹. The viscosity function of this PMA has four distinct regions that were described in the literature^[14] and are found in a variety of materials such as liquid crystals, mesophase carbon pitches^[15,16], liquid crystal polymers^[17-20], etc.

Regions of viscosity function can be seen on the example of 4% SBS PMA at 60°C. The first plateau (“Region 0”) ends at about 0.01 s⁻¹, where “Region 1” begins. Region 1 is the first shear-thinning region. This levels off to another (intermediate) plateau (“Region 2”). This begins at 0.1 s⁻¹; and, the last shear thinning (“Region 3”) starts at 1 s⁻¹.

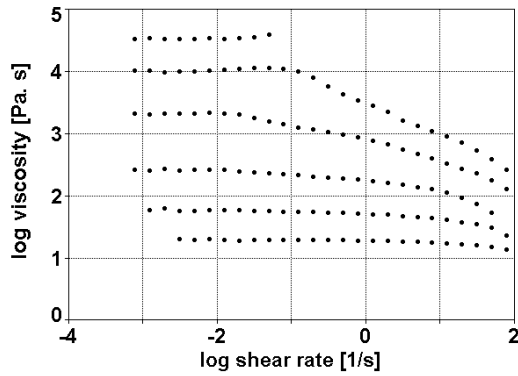


Figure 6: Viscosity function, 4% SBS PMA; T = 40°C, 50°C, 60°C, 70°C, 80°C, 90°C.

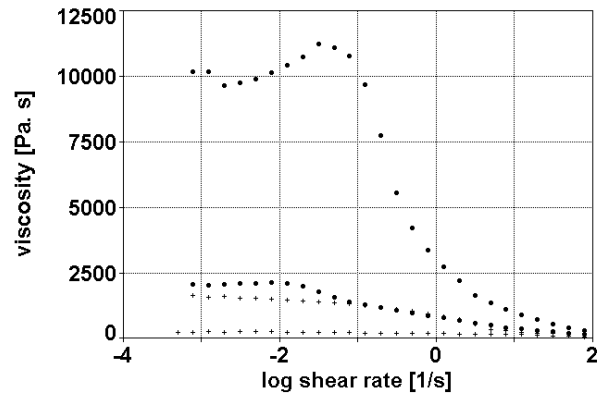


Figure 7: Viscosity function, 4% SBS PMA (•) and 4% EVA PMA (+); T = 50°C, 60°C.

Similar double-step shearing can also be observed in the blends of asphalt with four and more percent of the EVA copolymer, except that it is seen at higher temperatures. The viscosities of the 4% EVA PMA can be found in Figure 8, where four regions of the viscosity function appeared at 70°C, 80°C and 90°C. For clarity, these are portrayed in Figure 9 in a semi-log plot.

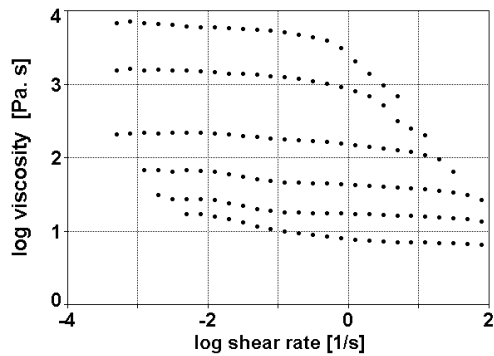


Figure 8: Viscosity function, 4% EVA PMA; T = 40°C, 50°C, 60°C, 70°C, 80°C, 90°C.

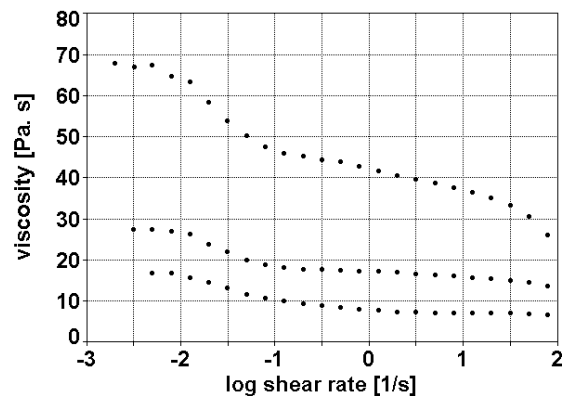


Figure 9: Viscosity function, 4% EVA PMA; T = 70°C, 80°C, 90°C.

Figure 10 displays the viscosities of the 8% SBS PMA, where four regions are observed at temperatures higher than 70°C.

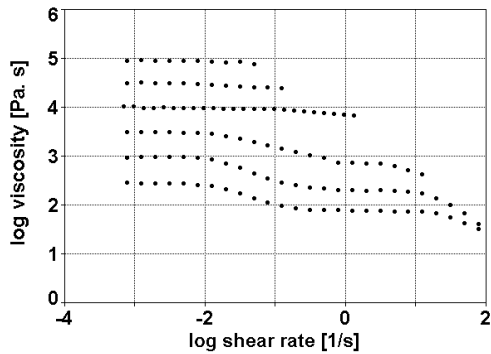


Figure 10: Viscosity function, 8% SBS PMA; T = 40°C, 50°C, 60°C, 70°C, 80°C, 90°C.

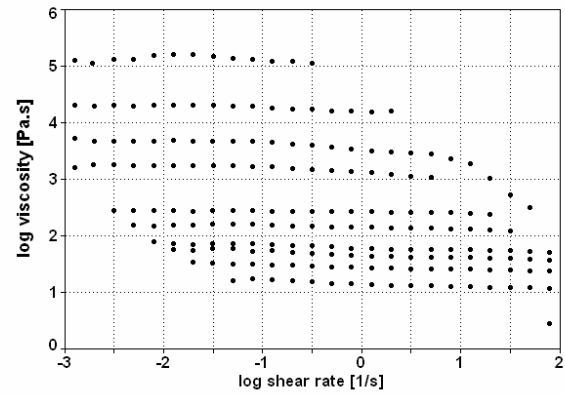


Figure 11: Viscosity function, 8% EVA PMA; T= 40°C, 50°C, 60°C, 70°C, 80°C, 90°C, 100°C, 110°C, 120°C, 130°C.

Figures 11 and 12 display the viscosities of the 8% EVA PMA. The semi-log plot in Figure 12 shows that these regions were shifted to even higher temperatures ($T \geq 100^\circ\text{C}$).

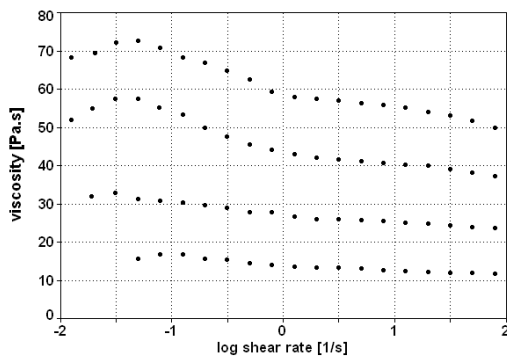


Figure 12: Viscosity function, 8% EVA PMA; T= 100°C, 110°C, 120°C, 130°C.

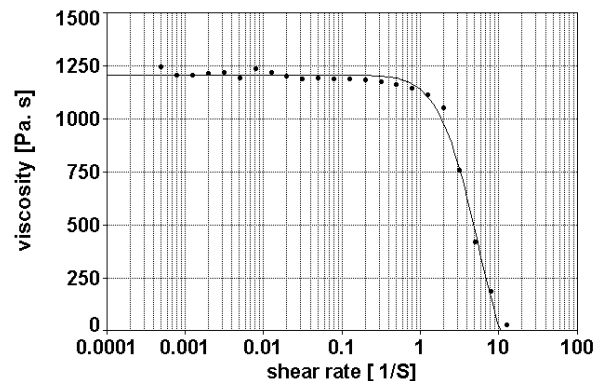


Figure 13: Viscosity fit, equation (6), base asphalt; T = 40°C.

The observed double-step shear thinning in the viscosity function of the studied PMAs is interesting and not yet quite understood. It is plausible to assume that the role of block copolymers is a deciding factor in this behaviour. These materials are known to form lamellae morphology^[21]. The shear-induced alignment together with the molecular architecture of the copolymer certainly play roles in the mechanical response of the network to the applied shear and also to the temperature.

The mesoscopic models of flow-aligning liquid crystals usually lead to the viscosity function expressed as a Carreau-Yashuda power law fluid^[22]. To describe a double-step shear-thinning viscosity function, the two terms have to be used^[23]. Even with two terms of the Carreau-Yashuda type, it is not possible to describe a shear-thickening part of the viscosity function, which is observed at some temperatures in some PMAs.

As the viscosity function revealed, the network found in PMAs studied here is weak and not permanent. The nonlinear generalization of Lodge's rubber-like liquid model^[25,26] was used to model

significant nonlinear effects in transient flows of PMAs^[24]. We can show that this model can simulate the above-described behaviour of the viscosity function.

Assume that the extra stress tensor, $\underline{\tau}$, in PMA is given as:

$$\underline{\tau} = \int_{-\infty}^t M(t-t', I, II) \underline{C}^{-1}(t') dt' \quad (2)$$

where, M is the nonlinear memory function, $\underline{C}^{-1}(t')$ is the relative Finger tensor, and I and II are the first two principal invariants of \underline{C}^{-1} .

For the sudden start of the simple shear (shear rate, $\dot{\gamma}$), the constitutive equation (2) yields the shear stress component:

$$\tau_{12} = \dot{\gamma} t \int_t^{\infty} M(s, |\dot{\gamma} t|) ds + \dot{\gamma} \int_0^t M(s, |\dot{\gamma} s|) ds \quad (3)$$

Note that, $I = II = 3 + (\dot{\gamma} t)^2$ for $t' < 0$, and $I = II = 3 + \dot{\gamma}^2 (t - t')^2$ for $t > t' > 0$.

We have found out that instead of using the usual time-strain factorization of the memory function, the transient shear experiments are better described in PMAs by the memory function written as:

$$M(s, \gamma) = \sum_{i=1}^N \mu_i(s) h_i(\gamma) \quad (4)$$

Hence each i -th relaxation mode has its own damping function, h_i . In equation (4), γ , is the strain and μ_i is the linear viscoelastic memory function of the i -th relaxation mode. Since the memory function μ_i is related to the relaxation function G_i (modulus) as,

$$\mu_i(s) = -\frac{dG_i(s)}{ds} \quad (5)$$

one can calculate the stress growth coefficient $\eta^+(t; \dot{\gamma}) = \tau_{12}(t) / \dot{\gamma}$ by knowing G_i and h_i . The shear viscosity function is simply the limit of η^+ for $t \rightarrow \infty$. Thus, for the simulation of the viscosity function one needs the input functions: $G_i(s)$ and $h_i(|\dot{\gamma} s|)$. For example, the Maxwell relaxation modes $G_i = g_i \exp(-s/\lambda_i)$

and the Osaki-Laun damping functions $h_i = k_i \exp(-\alpha_i |\dot{\gamma} s|) + (1 - k_i) \exp(-\beta_i |\dot{\gamma} s|)$ [27] yield:

$$\eta(\dot{\gamma}) = \sum_{i=1}^N \frac{g_i}{\lambda_i} \left[\frac{k_i}{A_i^2} + \frac{(1-k_i)}{B_i^2} \right] \quad (6)$$

Here,

$$A_i = \frac{1}{\lambda_i} + \alpha_i |\dot{\gamma}|, \quad B_i = \frac{1}{\lambda_i} + \beta_i |\dot{\gamma}| \quad (7)$$

are the reciprocal nonlinear relaxation times, now functions of the shear rate. With the set of input parameters $[g_i, \lambda_i, \alpha_i, \beta_i, k_i]_{i=1,2,\dots,N}$, one can fit the data of the shear viscosity function obtained in the base and polymer-modified asphalts. The results with only two relaxation modes are shown in Figures 13-16, where the basic types of the viscosity function observed in the studied asphalts are fitted to equation (6).

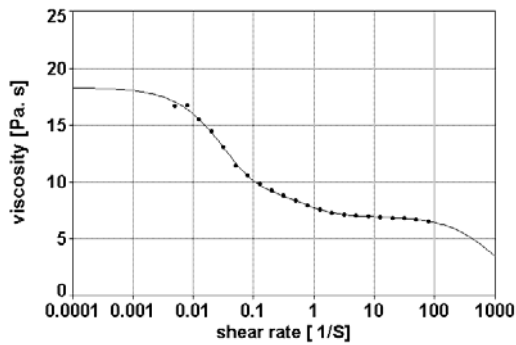


Figure 14: Viscosity fit, equation (6), 4% EVA PMA; T = 70°C.

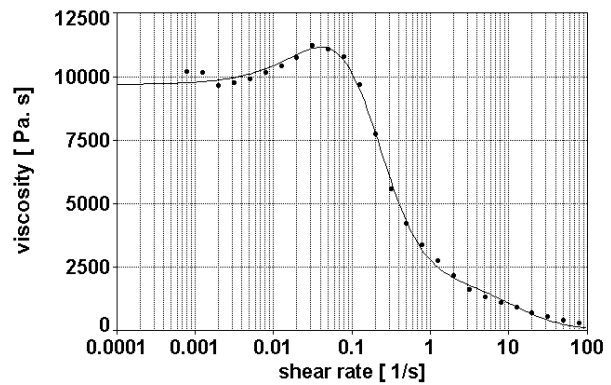


Figure 15: Viscosity fit, equation (6), 4% SBS PMA; T = 50°C.

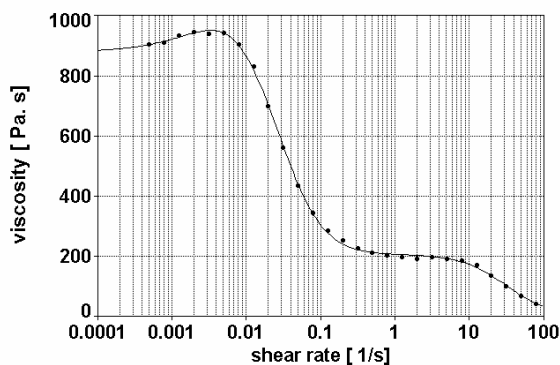


Figure 16: Viscosity fit, equation (6), two modes, 8% SBS PMA; T = 80°C.

As can be seen from Figures 13-16, the presented nonlinear model fits the viscosities very well and can even capture all nonlinear effects, such as the shear thickening at certain temperatures.

Conclusions

It was observed that the flow behaviour of polymer-modified asphalt is different from the one of base asphalt. This difference (peculiar behaviour of viscosity function of PMAs) is better captured by steady shear measurements than by dynamic measurements.

The construction of the master curves from the dynamic (oscillation) measurements did not show a significant difference between the base and polymer-modified asphalts, as the viscosity function did.

When the viscosity function was investigated, it revealed some nonlinear effects that dynamic measurements could not. The observed "anomalous" behaviour of the viscosity function is probably caused by rearrangement of the polydomain structures accompanied by detachment of flexible chains, which can temporarily join some domains.

The interrupted shear experiments, and also the investigation of the shear creep, in the discussed materials point to a structure that is time dependent. We were able to model this type of nonlinear behaviour successfully with the nonlinear generalization of Lodge's rubber-like liquid model.

Acknowledgements

The authors express their gratitude to the Natural Sciences and Engineering Research Council of Canada and to Husky Energy Ltd. for their financial support of this work.

References

- [1] Lian H., Lin J.R., and Yen T.F. (1994), *Fuel*, **73**, 423-428.
- [2] Dickie J.P., Haller H.N., and Yen T.F. (1969), *Journal of Colloid and Interface Science*, **29**, 475-484.
- [3] Yen T.F., Erdman J.G., and Pollack S.S. (1961), *Analytical Chemistry*, **11**, 1587-1594.
- [4] Yen, T.F. (1973), *Fuel*, **52**, 93-98.
- [5] Yen T.F. (1971), *Nature Phys. Sci.*, **233**, 9-13.
- [6] Khakimullin Y.N., Kimel'blat V.I., and Chebotareva I.G. (2000), *Mechanics of Composite Materials*, **36 (5)**, 417-22.
- [7] Collins J.H., Bouldin M.G., Gelles R., and Berker A. (1991), *Proceeding of the Association of Asphalt Paving Technologists*, **60**, 43-79.
- [8] Valkering C.P., Vonk W.C., and Whiteoak C.D. (1992), *Shell Bitumen Review*, **66**, 9-11.
- [9] Polacco G., Stastna J., Vlachovicova Z., Biondi D., and Zanzotto L. (2004), *Polymer Engineering and Science*, **44 (12)**, 2185-2193.
- [10] Ettre, F.D., and Snell, L.S. (1971), *Encyclopedia of Chemical Analysis*, **12**, 349-361, John Wiley and Sons Inc.
- [11] Anderson D.A., Christensen D.W., Roque R., and Robyak R.A. (1992), *Proc. ASTM STP*, 1108.
- [12] Ferry J.D. (1980), *Viscoelastic Properties of Polymers*, Wiley, New York.
- [13] Baumgaertel M., and Winter, H.H. (1989), *Rheological Acta*, **28**, 119-144.
- [14] Sigillo I., Grizutti N. (1994), *Journal of Rheology*, **38**, 589-599.
- [15] Onogi, S., Asada, T., Astarita, G., Marrucci, G., and Nicolais, I. (eds.) (1980), *Proc. of the VIII Int. Congress on Rheol.*, Plenum, New York.
- [16] Cato, A.D., and Edie D.D. (2003), *Carbon*, **41**, 1411-1417.
- [17] Kiss G. and Porter R.S. (1996), *Journal of Polymer Science: Part B: Polymer Physics*, **34**, 2271-2289.
- [18] Suto S. M., Ito O.R., and Karasawa M. (1987), *Polymer*, **28**, 23-32.
- [19] Magda J.J., Baek S.G., and De Vries K. L. (1991), *Macromolecules*, **24**, 4460-4468.
- [20] Sigillo I., Grizutti N. (1994), *J. Rheol.*, **38**: 589-599.
- [21] Phatak A., Macosko C.V., and Bates F.S. (2005), *J. Rheol.*, **49**, 197-214.
- [22] Grecov D., and Rey A.D. (2002), *Mol. Cryst. Liq. Cryst.*, **391**, 57-94 .
- [23] Stastna J., Zanzotto L., and Vacin O. (2003), *Journal of Colloid and Interface Science*, **259**, 200-207.
- [24] Wekumbura C., Stastna J., Zanzotto L. (2005), *Materials and Structures*, **38**, in press.
- [25] Lodge, A.S. (1964) *Elastic Liquids*, Academic Press, London, UK.
- [26] Wagner, M.H. (1976), *Rheol. Acta*, **15**: 136-142.
- [27] Osaki K., Ohta S., Fukuda M. And Kurata M., (1976), *Journal of Polymer Science: Polymer Physics Edition*, **17**: 1701-1715.